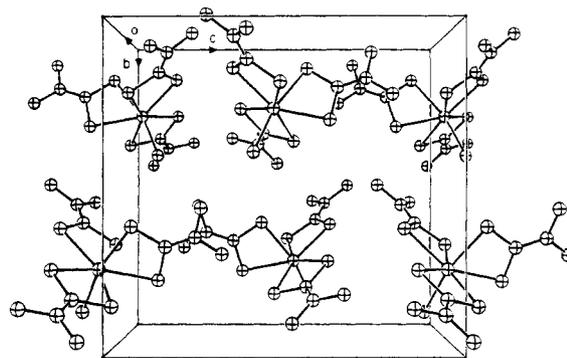closer to the chlorine atom, while ring a is folded in the direction of ring c. The dihedral angles between the ligand planes and the appropriate S–Ti–S group are 2.9, 2.3, and 5.5° for rings a, b, and c, respectively; the corresponding displacements of the Ti(IV) atom from the ligand planes are 0.10, 0.04, and 0.19 Å, respectively. The departures from planarity are probably due to crystal packing; there are a number of relatively close intermolecular contacts but none is more than 0.2 Å less than the sum of the van der Waals radii. A packing diagram is presented in Figure 3.

Figure 3. Model in perspective to illustrate the packing of Ti[S₂-CN(CH₃)₂]₃Cl molecules in the crystalline arrangement. One unit cell is outlined. The view is perpendicular to the (100) plane.

Supplementary Material Available. A listing of structure factor amplitudes will appear following these pages in the microfilm edition of this volume of the journal. Photocopies of the supplementary material from this paper only or microfiche (105 × 148 mm, 24× reduction, negatives) containing all of the supplementary material for the papers in this issue may be obtained from the Journals Department, American Chemical Society, 1155 16th St., N.W., Washington, D. C. 20036. Remit check or money order for $3.00 for photocopy or $2.00 for microfiche, referring to code number JACS-74-3843.

Electronic Structure of Square-Planar Transition Metal Complexes. I. The PtCl₄²⁻ and PdCl₄²⁻ Ions

R. P. Messmer,*[1a] L. V. Interrante,[1a] and K. H. Johnson[1b]

Contribution from General Electric Corporate Research and Development, Schenectady, New York 12301, and the Department of Metallurgy and Materials Science, Massachusetts Institute of Technology, Cambridge, Massachusetts 02139. Received January 8, 1974

Abstract: Molecular orbital calculations using the self-consistent-field Xα-scattered wave (SCF-Xα-SW) method have been carried out for the PtCl₄²⁻ and PdCl₄²⁻ ions. Optical transitions have been calculated and found to be in good agreement with the experimental absorption spectra. The calculated d-level ordering for these two complexes is $d_{x^2-y^2} > d_{xy} > d_{xz}, d_{yz} > d_{z^2}$, and the mixing among d orbitals and ligand orbitals is predicted to be considerably stronger than in previous calculations.

The electronic structure of square-planar transition metal complexes remains a topic of continuing interest and controversy, in spite of numerous spectral,[2–8] magnetic circular dichroism,[9,10] and photoelectron[11–13]

(1) (a) General Electric. (b) Massachusetts Institute of Technology.

(2) D. S. Martin, Jr., M. A. Tucker, and A. J. Kassman, *Inorg. Chem.*, 4, 1682 (1965); 5, 1298 (1966).

(3) P. Day, A. F. Orchard, A. J. Thomson, and R. J. P. Williams, *J. Chem. Phys.*, 42, 1973 (1965).

(4) O. S. Mortensen, *Acta Chem. Scand.*, 19, 1500 (1965).

(5) D. S. Martin, Jr., *Inorg. Chim. Acta Rev.*, 5, 107 (1971).

(6) H. H. Patterson, J. J. Godfrey, and S. M. Khan, *Inorg. Chem.*, 11, 2872 (1972).

(7) M. L. Morreau-Colin, *J. Chim. Phys. Physicochim. Biol.*, 67, 498 (1970).

(8) W. R. Mason, III, and H. B. Gray, *J. Amer. Chem. Soc.*, 90, 5721 (1968).

(9) D. S. Martin, Jr., J. G. Foss, M. E. McCarville, M. A. Tucker, and A. J. Kassman, *Inorg. Chem.*, 5, 491 (1966).

(10) (a) A. J. McCaffery, P. N. Schatz, and P. J. Stephens, *J. Amer. Chem. Soc.*, 90, 5730 (1968); (b) S. B. Piepho, P. N. Schatz, and A. J. McCaffery, *ibid.*, 91, 5994 (1969).

(11) D. Cahen and J. E. Lester, *Chem. Phys. Lett.*, 18, 108 (1973).

(12) W. E. Moddeman, J. R. Blackburn, G. Kumar, K. A. Morgan, R. G. Albridge, and M. M. Jones, *Inorg. Chem.*, 11, 1715 (1972).

(13) P. Biloen and R. Prins, *Chem. Phys. Lett.*, 16, 611 (1972).

studies and many theoretical investigations.[14–19] The controversy centers mainly on the ordering of the d-orbital energy levels in the various complexes, although definitive answers to questions such as the degree of covalency in the metal–ligand bonds and the amount of π-bonding occurring in such systems have yet to be presented.

In addition to the continuing interest in these complexes as molecular entities with their own characteristic spectral and chemical behavior, a more recent impetus to study the electronic structure of these complexes results from the unusual solid-state properties observed in certain crystalline compounds such as Pt(NH₃)₄Pt-

(14) R. F. Fenske, D. S. Martin, Jr., and K. Reudenberg, *Inorg. Chem.*, 1, 441 (1962).

(15) W. Th. A. M. van der Lugt, *Chem. Phys. Lett.*, 10, 117 (1971); *Int. J. Quantum Chem.*, 6, 859 (1972).

(16) H. Basch and H. B. Gray, *Inorg. Chem.*, 6, 365 (1967).

(17) J. Demuynck, A. Veillard, and U. Wahlgren, *J. Amer. Chem. Soc.*, 95, 5563 (1973).

(18) J. Demuynck, A. Veillard, and G. Vinot, *Chem. Phys. Lett.*, 10, 522 (1971).

(19) L. V. Interrante and R. P. Messmer, *Inorg. Chem.*, 10, 1174 (1971).

Cl_4[20] and $K_2[Pt(CN)_4]Br_{0.3} \cdot 3H_2O$.[21] In these compounds the planar units are stacked in a columnar, quasi-one-dimensional array with close metal–metal separations. The large anisotropy in the optical and electrical properties of these solids suggests that there is considerable interaction between the units. A basic understanding of the nature of these solid-state interactions and their relationship to the observed properties requires much more definitive information regarding the electronic structure of the component planar complex units than is presently available.

Previous theoretical discussions of the electronic structure of square-planar transition metal complexes have included calculations using crystal field theory,[2,14] iterative extended Hückel methods (IEH),[16,22] a "revised INDO procedure,"[15] as well as ab initio limited basis set Hartree–Fock calculations.[18,23,24] A brief comparison of these various methods to each other and to the self-consistent-field $X\alpha$-scattered wave (SCF-$X\alpha$-SW) approach used in this work is presented below.

Comparison of Theoretical Methods

Historically, the crystal field theory was the first theoretical treatment used to attempt a quantitative description of certain spectral information in transition metal complexes. It has been used extensively in the study of planar complexes and has provided much useful information regarding the low energy d → d transitions in such systems. Its usefulness has been mainly limited, however, to complexes whose metal–ligand bonding is largely ionic; furthermore, even in these cases it can say nothing about the important charge transfer transitions.

The other types of calculations mentioned above are all capable of describing charge transfer transitions, since they are molecular orbital approaches based on the linear combination of atomic orbitals (LCAO) approximation; however, each has its own set of problems. For ab initio LCAO–MO computations the number of two-electron integrals which must be calculated increases as N^4, where N is the number of basis functions included. Thus the chief motivation for using semiempirical schemes such as IEH methods or INDO is to avoid the evaluation of many integrals by making various approximations and incorporating experimental atomic data.

Of the semiempirical schemes, the IEH methods have been the most frequently applied and have been widely used as a guide to the experimentalist as well as for providing qualitative information about bonding, charge distributions, nature of d → d and charge transfer transitions, etc. However, from a quantitative point of view, they have not been very reliable. Moreover, the degree of parameterization required, not to mention the often fragmentary nature of the experimental data used as a basis for this parameterization, raises some serious questions in certain cases as to the significance—even in a qualitative way—of the results of such calculations. In addition, there is considerable difficulty in justifying the approximations which are made, on theoretical grounds. A recently suggested modified INDO method,[15] which is considerably more troublesome to implement than the IEH methods, yields transition energies for charge-transfer transitions but fails to provide a reasonable description for the d → d transitions. Hence, its advantage over the IEH methods is questionable.

The principal difficulty of ab initio LCAO–MO calculations is the "N^4 problem" mentioned above. Thus in order to make a calculation practical for transition metal systems, limited basis sets must be employed. This in turn, however, poses another problem which is illustrated by two recent ab initio calculations using limited basis sets of different quality[23,24] for the Ni-$(CN)_4{}^{2-}$ complex. Not only are the orbital energies different but their ordering is also different.

A further problem illustrated by the Ni(CN)$_4{}^{2-}$ calculations[23,24] and discussed thoroughly in the work of Demuynck and Veillard[23] is the fact that Koopmans' theorem is not valid for such d^8 square-planar ions; i.e., the sequence of ionization potentials (computed as the difference in total energies between the dinegative and the appropriate mononegative ions) is different from the sequence of orbital energies.

We will show in this paper, using two examples of square-planar complexes, that the use of Slater's $X\alpha$ theory based on a local approximation to exchange correlation, instead of Hartree–Fock theory, leads to a set of one-electron orbitals which are susceptible to the chemists' usual concepts regarding them, and thus one need not give up the one-electron orbital scheme as a means of deriving and assigning electronic transitions. Furthermore, when the $X\alpha$ theory is implemented using Johnson's scattered wave (SW) approach to molecular orbital theory, the usual basis set difficulties and the two-electron integral problem of the usual LCAO approach to molecular orbital theory are eliminated. The combination yields the SCF-$X\alpha$-SW method which allows quantitative calculations on transition metal complexes to be carried out in a fraction of the computation time necessary for the ab initio LCAO method.

The SCF-$X\alpha$-SW method has been successfully applied recently to a wide variety of tetrahedral and octahedral transition metal complexes to provide interpretations and assignments of optical spectra and X-ray photoemission (ESCA) spectra. In the next section we will briefly outline the main features of the SCF-$X\alpha$-SW method.

Method of Calculation

Only a brief summary of the most pertinent aspects of the SCF-$X\alpha$-SW method will be given here. The $X\alpha$ theory—also referred to as the Hartree–Fock–Slater method—has been reviewed recently by Slater,[25] and Johnson[26] has recently reviewed the scattered wave approach to the solution of the $X\alpha$ equations.

In the $X\alpha$ theory as in the Hartree–Fock theory, one has a set of one-electron integro–differential equations which must be solved self-consistently in order to obtain the molecular orbitals. The essential differences arise in the expressions for the total energy and exchange potential. The expressions for the total energy

(20) F. Mehran and B. A. Scott, *Phys. Rev. Lett.*, **31**, 99 (1973); L. V. Interrante, *J. Chem. Soc., Chem. Commun.*, 302 (1972).
(21) H. R. Zeller, *Advan. Solid State Phys.*, **13**, 31 (1973).
(22) F. A. Cotton and C. B. Harris, *Inorg. Chem.*, **6**, 369 (1967).
(23) J. Demuynck and A. Veillard, *Theor. Chim. Acta*, **28**, 271 (1973).
(24) I. H. Hillier and V. R. Saunders, *Mol. Phys.*, **22**, 1025 (1971).

(25) J. C. Slater, *Advan. Quantum Chem.*, **6**, 1 (1972).
(26) K. H. Johnson, *Advan. Quantum Chem.*, **7**, 143 (1973).

and exchange potential (for a closed shell system) in Hartree–Fock theory are given by eq 1 and 2, respectively.

$$\langle E_{\mathrm{HF}}\rangle = \sum_i I_{ii} + \frac{1}{2}\sum_{ij}(J_{ij} - K_{ij}) \qquad (1)$$

$$V_{\mathrm{HF}}{}^{\mathrm{ex}}(j) = \int \frac{2P_{12}}{r_{12}}\phi_j{}^*(2)\phi_j(2)\mathrm{d}v_2 \qquad (2)$$

$$K_{ij} = \langle\phi_i|V_{\mathrm{HF}}{}^{\mathrm{ex}}(j)|\phi_j\rangle$$

tively. The corresponding expressions for the case of the Xα theory are given in eq 3 and 4. In the above

$$\langle E_{\mathrm{X}\alpha}\rangle = \sum_i n_i I_{ii} + \frac{1}{2}\sum_{ij}n_i n_j J_{ij} + \frac{1}{2}\sum_i n_i K_{ii} \qquad (3)$$

$$V_{\mathrm{X}\alpha}{}^{\mathrm{ex}} = -9\alpha[(3/4\pi)\rho]^{1/3}$$

$$K_{ii} = \langle\phi_i|V_{\mathrm{X}\alpha}{}^{\mathrm{ex}}|\phi_i\rangle \qquad (4)$$

expressions, the sums are over all occupied spin orbitals. The integrals, I_{ii}, represent the contributions to the total energy from one-electron operators; the J_{ij} are coulomb integrals. P_{12} in eq 2 represents the permutation operator which exchanges the coordinates of electrons 1 and 2. In eq 4, ρ is the electronic charge density given by $\rho = \Sigma_i n_i \phi_i{}^*\phi_i$, where the ϕ_i are the one-electron spin orbitals. The unit of energy for the above equations is the rydberg. It should be noted that, whereas the Hartree–Fock exchange is nonlocal, the Xα exchange is local and proportional to the cube root of the charge density. The α is a constant which will be discussed shortly. Although the use of such a local exchange potential is relatively new in the theoretical treatment of molecules, it has long been used very successfully in solid-state physics for the calculation of electronic structures. The other difference which should be pointed out is that the Xα total energy, $\langle E_{\mathrm{X}\alpha}\rangle$, is in general a function of the occupation numbers, n_i, and that a single expression, eq 4, describes the total energy for spin-restricted calculations. In spin-restricted Hartree–Fock theory, eq 2 is correct for closed-shell systems only; in open shell systems rather complicated expressions obtain, whose form depends upon the particular open-shell situation.

At first sight these differences may not appear to be very important; they are, however, of extreme importance both from a practical computational view and from the view of basic physical content. As regards physical content, a brief outline of the Xα theory is provided.

(1) Koopmans' theorem is not valid; however, Slater's transition-state concept[25] applies. This is an advantage since the transition state allows one to interpret electronic transitions in terms of one-electron orbitals and yet includes electronic relaxation. Its reliability and accuracy far surpass the Koopmans' theorem of Hartree–Fock theory; furthermore, it is often found that the latter is not even a meaningful approximation in certain cases.

(2) Fermi statistics are obeyed. That is, no orbital is ever occupied which has a higher energy than a lower lying empty (or partially occupied) orbital. The fact that this is not the case in Hartree–Fock theory often leads to problems of convergence of the SCF equations, as well as to difficulties in interpretation.

(3) The virial theorem and Hellmann–Feynmann

theorem are rigorously satisfied for the Xα method when a single α value is used for the electronic system. They are of course in principle also satisfied for Hartree–Fock theory, although rarely in practice for anything but the simplest systems.

(4) The unoccupied orbitals (or virtual orbitals) of Xα theory have a physical significance and can be used directly to discuss excitations of the electronic system because the same potential, due to the $N - 1$ other electrons, is seen by both occupied and unoccupied orbitals; this is in contrast to the Hartree–Fock theory where occupied orbitals experience a potential due to the $N - 1$ other electrons, whereas unoccupied orbitals experience a potential more appropriate to N other electrons.

The scattered wave formalism[26] provides a very accurate approximate method for solving the Xα SCF equations. By way of analogy, one may say that the scattered wave (SW) formalism is to the Xα theory what the LCAO formalism of Roothaan[27] is to Hartree–Fock theory. One may of course use the LCAO approximation to solve the Xα equations and indeed this has been done in conjunction with the discrete variational method[28] which uses direct numerical integration. However, the SW method provides many advantages over the LCAO approach as will become clear later.

In the scattered wave method, the space occupied by a molecule is divided into three regions. Region I consists of spherical volumes located about the centers of the respective atoms, so constructed that the spheres are tangent to one another. Region II is the volume outside the atomic spheres and inside an "outer sphere" which surrounds the molecule and is centered at the molecular center and is constructed to be tangent to the atomic spheres at the extremities of the molecule. Region III is the space outside the outer sphere.
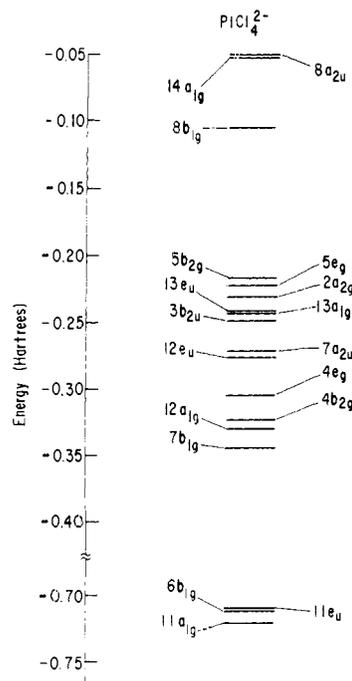
This division of space allows one to approximate the complete Xα potential by a potential which is spherically averaged within each atomic sphere and outside the outer sphere and volume averaged in region II. With this form of the potential one can obtain, by partial wave expansions, exact solutions of the resulting one-electron Schrödinger equations in the three regions of space. It has also recently been shown that one may use overlapping atomic spheres since the various expansion theorems are still valid, so long as the atomic sphere centered on any one atom has a radius which is less than the internuclear separations with respect to its neighbors.[29]

The one-electron equations for a given orbital in each region of space are a function of an energy parameter, E. For an arbitrary value of this parameter, the solutions in the three regions of space will not connect properly; i.e., the orbital will not be continuous and have a continuous first derivative across the various boundaries. Hence, for an arbitrary value of E a proper solution of the one-electron Schrödinger equation is not obtained. The value of E for which the orbital has a continuous value and first derivative across the boundaries is the eigenvalue or orbital energy.

(27) C. C. J. Roothaan, *Rev. Mod. Phys.*, **23**, 69 (1951).
(28) D. E. Ellis and G. S. Painter, *Phys. Rev. B*, **2**, 2887 (1970).
(29) N. Rösch, W. G. Klemperer, and K. H. Johnson, *Chem. Phys. Lett.*, **23**, 149 (1973).

$PtCl_4^{2-}$

Energy (Hartrees)

-0.05 — $14a_{1g}$ ⋯⋯ $8a_{2u}$

-0.10 — $8b_{1g}$ ⋯⋯

-0.15 —

-0.20 — $5b_{2g}$ ═══ $5e_g$
$13e_u$ ═══ $2a_{2g}$
-0.25 — $3b_{2u}$ ═══ $13a_{1g}$
$12e_u$ ═══ $7a_{2u}$
$4e_g$
-0.30 — $4b_{2g}$
$12a_{1g}$ ═══
$7b_{1g}$ ═══
-0.35 —

-0.40 —
≈
-0.70 — $6b_{1g}$ ═══
$11a_{1g}$ ═══ $11e_u$
-0.75 —

Figure 1. Ground-state SCF-Xα electronic energy levels of $PtCl_4^{2-}$ in the approximate stabilizing electrostatic field of the K_2PtCl_4 crystalline environment. The highest occupied orbital is $5b_{2g}$.

Thus in the SW method, the one-electron equations are implicit functions of the parameters (E_i), and the secular equation is obtained by imposing the conditions of continuity for the orbital functions and their first derivatives across the spherical boundaries. The value of the determinant of the secular equation will then vanish for an eigenvalue of the system.[26]

The energies of optical and X-ray photoemission transitions may be calculated within the SCF-Xα-SW method by using Slater's transition-state concept.[25] The latter allows one to obtain very good approximations to the differences between the total ground-state energy and those of excited states. The excitation of an electron from orbital a to orbital b is described by taking half an electron from orbital a and putting it into orbital b and then solving self-consistently for the new one-electron level positions. Such a transition-state calculation allows for the effects of orbital relaxation and gives the excitation energy as the difference of the new one-electron energy level positions of orbitals a and b. Spin polarized (or spin unrestricted) calculations[25] may also be performed, and in the case of complexes of D_{4h} symmetry by combining the results with the spin restricted calculations one may obtain approximations to both the singlet and triplet excited states in a way previously described.[30]

Computational Details

Schwarz[31] has shown for atoms that the optimal value of α, the exchange parameter, depends in a systematic way upon the atomic number. He has tabulated the values of α for elements up to Nb. His values of α are used in the appropriate atomic spheres, and, for Pt and Pd, extrapolations of his values to these higher atomic

(30) R. P. Messmer, U. Wahlgren, and K. H. Johnson, *Chem. Phys. Lett.*, 18, 7 (1973); R. P. Messmer, *Int. J. Quantum Chem.*, 7S, 371 (1973).
(31) K. Schwarz, *Phys. Rev. B*, 5, 2466 (1972).

numbers are used. The value of α in the intersphere region (region II) is taken as the weighted average of the appropriate atomic α's. The values of the various atomic sphere radii used in the calculations are determined by requiring (for the MCl_4^{2-} complexes) that the ratio of the sphere radii (r_M/r_{Cl}) be equal to the ratio of their Slater atomic radii[32] and that their sum $(r_M + r_{Cl})$ be equal to the observed internuclear separation.

In solution or in a solid, complex ions such as $PtCl_4^{2-}$ are stabilized by an electrostatic potential provided by the surrounding medium. This potential can be quite well approximated by surrounding the ion by a sphere (a so-called Watson sphere[33]) with a charge opposite to that of the ion and with a radius which is chosen, for example, to approximate the Madelung potential supplied by the surrounding crystalline environment.

Results

$PtCl_4^{2-}$. For the SCF-Xα-SW model applied to $PtCl_4^{2-}$, the Pt–Cl bond length was taken as 4.38 bohr (2.32 Å);[34] the atomic sphere radii of Pt and Cl and the outer sphere radius were taken as 2.53, 1.87, and 6.29 bohr, respectively. The stabilizing electrostatic field of the crystalline environment, K_2PtCl_4, was approximated by surrounding the $PtCl_4^{2-}$ cluster with a Watson sphere centered on Pt with a radius of 6.67 bohr and having a charge of $+2$ electrons on its surface. The value of α for the Pt atomic sphere was 0.70000 and for Cl, 0.72325;[31] the value of α in the inter and outer sphere regions was 0.71860.

The orbital energy diagram which results from a spin-restricted solution is shown in Figure 1. The atomic contributions to the orbitals are displayed in Table I, where for each MO the fraction of the electronic

Table I. Molecular Orbital Charge Distributions for $PtCl_4^{2-}$ [a]

| | % of orbital charge | | | |
Orbital	Pt	Cl	Inner sphere	Outer sphere
$5b_{2g}$	50.3	7.5	17.4	2.4
$5e_g$	38.7	9.8	20.9	1.4
$2a_{2g}$	0.0	17.3	27.4	3.4
$13e_u$	1.6	16.4	29.4	3.4
$13a_{1g}$	58.6	3.5	26.4	1.2
$3b_{2u}$	0.0	16.3	32.0	2.9
$7a_{2u}$	1.0	14.2	40.4	2.0
$12e_u$	3.2	14.6	38.0	0.3
$4e_u$	52.6	5.9	23.0	0.8
$4b_{2g}$	42.2	7.4	27.1	1.4
$12a_{1g}$	38.1	9.9	20.1	2.4
$7b_{1g}$	48.1	8.6	14.4	2.9

[a] The % charge for Cl is the % charge contained in *one* Cl sphere. In the case of degenerate orbitals, the charge quoted represents the average over the degenerate partners.

charge contained in the atomic spheres, the inter sphere region, and the outer sphere region is listed.

From Table I it is clear that there is considerable mixing between d orbitals and ligands; this is considerably stronger than that obtained in most previous calculations, although the results of Basch and Gray[16] provide a striking exception in their similarity to the

(32) J. C. Slater, "Quantum Theory of Molecules and Solids," Vol. 2, McGraw-Hill, New York, N. Y., 1965, p 54.
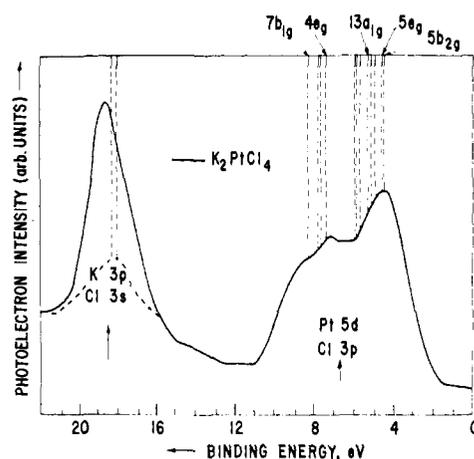(33) R. E. Watson, *Phys. Rev.*, 111, 1108 (1958).
(34) H. J. M. Bowen, *Chem. Soc., Spec. Publ.*, No. 11 (1958).
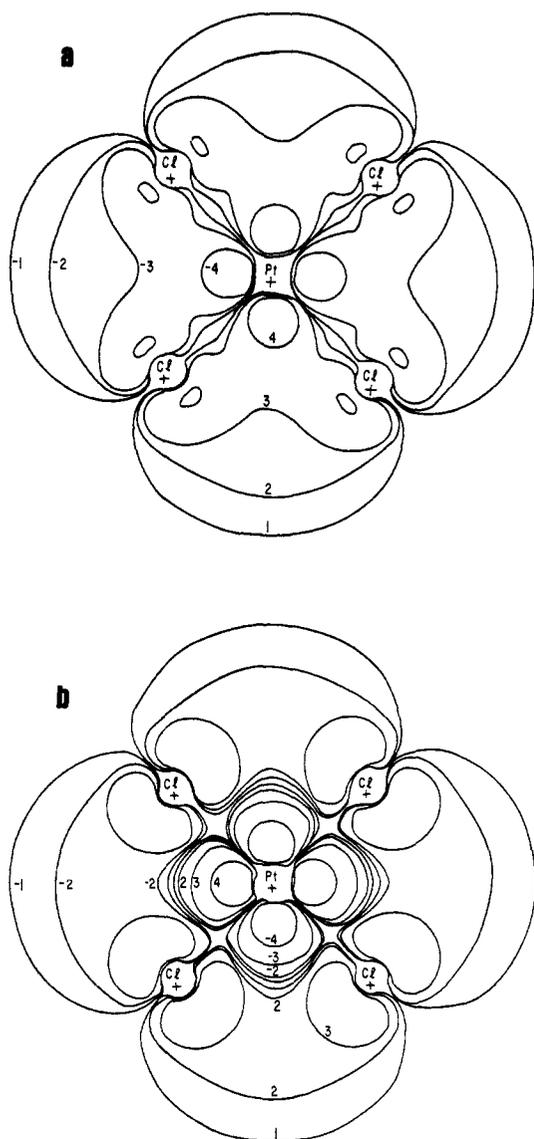
Figure 2. Contour plots of two orbitals in $PtCl_4^{2-}$. The contour values increase in absolute magnitude with increasing absolute values of the contour labels. The sign of the labels gives the sign of the orbital lobes. The interior nodes at the various atoms are not shown for clarity of presentation: (a) the $4b_{2g}$ bonding orbital showing the mixing between the metal and ligands, (b) the $5b_{2g}$ antibonding orbital, again showing appreciable metal and ligand components.

Figure 3. Calculated transition-state energies superimposed on the experimental X-ray photoemission results of Biloen and Prins (cf. ref 13).

present calculations. This metal–ligand interaction is illustrated in Figure 2 where the wave functions for the $5b_{2g}$ and $4b_{2g}$ orbitals are shown. Figure 2b shows the antibonding $5b_{2g}$ orbital, which in the calculations of Cotton and Harris is almost exclusively an atomic d_{xy} orbital. The bonding $4b_{2g}$ orbital is shown in Figure 2a, again demonstrating the significant metal–ligand interaction. Along with this stronger metal–ligand mixing the d-like orbitals are not energetically separated from the ligand orbitals as is usually supposed but are found in the same energy region (e.g., note the positions of the ligand $13e_u$ and $2a_{2g}$ orbitals in Figure 1). This situation must clearly be taken into account in discussing the low energy electronic absorption spectrum of the $PtCl_4^{2-}$ ion. This point will be returned to later in the discussion.

As far as the "d-like" molecular orbitals are concerned, the ordering $8b_{1g}(d_{x^2-y^2}) > 5b_{2g}(d_{xy}) > 5e_g$-

$(d_{zz},d_{yz}) > 13a_{2g}(d_{z^2})$ is the same as "alternative A" proposed earlier by Martin, et al.,[2] on the basis of experimental observations and obtained from IEH calculations by Basch and Gray[16] and Cotton and Harris.[22]

It differs markedly from the ordering obtained by van der Lugt in his recent "revised INDO" semiempirical calculation,[15] which was $d_{z^2} > d_{zz}$, $d_{yz} > d_{xy}$. A further point about the latter calculation is that it concluded that the lower-lying b_{2g}, e_g, and a_{1g} orbitals (corresponding to the $4b_{2g}$, $4e_g$, and $12a_{1g}$ levels of Figure 1) are over 90% d-like in character and that the higher levels of these symmetries (corresponding to the $5b_{2g}$, $5e_g$, and $13a_{1g}$ levels of Figure 1) are almost exclusively p-like. This led van der Lugt to suggest that if Koopmans' theorem is valid, X-ray photoelectron spectroscopy (XPS) should show the electrons of lowest ionization potentials to be from orbitals of mainly ligand character. In fact, a subsequent XPS study of K_2PtCl_4 and Na_2PtCl_4 by Biloen and Prins[13] has clearly shown that, to the contrary, the most weakly bound electrons have substantial d character.

The experimental data for K_2PtCl_4 are shown in Figure 3. The peak between 15–20 eV has contributions from both the Cl 3s and K 3p electrons. The Cl 3s contribution was determined from experiments on the Na_2PtCl_4 salt. The arrows at $\sim$18.5 and at 6.5 eV indicate the binding energies of the K 3p and Cl 3p electrons in KCl. The arrow at $\sim$6.5 eV indicates the region in which one would expect to find the Cl 3p nonbonding electrons in $PtCl_4^{2-}$.

Superimposed on the experimental data of Figure 3 are the transition-state ionization energies as determined from the SCF-Xα-SW calculations. Only those orbitals which have appreciable d character are labeled in Figure 3. The main features of the spectrum as determined by the calculations are (i) the peak at $\sim$5 eV is due mainly to antibonding orbitals containing an admixture of Pt 5d and Cl 3p character, (ii) the intensity at $\sim$5–6 eV is chiefly a consequence of nonbonding Cl 3p orbitals, (iii) the peak at $\sim$7 eV arises from bonding orbitals containing mainly admixtures of Pt 5d and Cl 3p character, and (iv) the peak at $\sim$18 eV is due to atomic-like Cl 3s orbitals.

In Table II, the calculated transition-state energies for the optical transitions in $PtCl_4^{2-}$ are listed and com-

Table II. Theoretical and Experimental Transition Energies (in eV) for $PtCl_4{}^{2-}$

Experiment[a,c]	Transition-state calculation	Transition	BG[a]	DSW[b]	M[c]
2.2			^3E_g	$^3A_{2g}$	$^3A_{2g}$
2.6[d]	3.0	$5e_g \rightarrow 8b_{1g}{}^f$	$^3A_{2g}$	^3E_g	^3E_g
3.0[d]	2.9	$5b_{2g} \rightarrow 8b_{1g}(^3A_{1g}' + {}^3E_g')$	$^3B_{1g}$	$^3B_{1g}$	
3.3[d]	3.5	$5b_{2g} \rightarrow 8b_{1g}(^1A_{2g})$	$^1A_{2g}$	$^1A_{2g}$	$^1A_{2g}$
	3.6	$13a_{1g} \rightarrow 8b_{1g}(^3B_{2g}' + {}^3E_g')$			
3.7[d]	3.8	$5e_g \rightarrow 8b_{1g}(^1E_g)$	^1E_g	^1E_g	^1E_g
4.5	4.4	$13a_{1g} \rightarrow 8b_{1g}(^1B_{1g})$	$^1B_{1g}$	$^1B_{1g}$	$^1B_{1g}$
5.0–5.4[e]	4.6	$13e_u \rightarrow 8b_{1g}(^1E_u)$			^1E_u
	4.8	$3b_{2u} \rightarrow 8b_{1g}(^1A_{2u})$			$^1A_{2u}$
	5.5	$12e_u \rightarrow 8b_{1g}(^1E_u)$	^1E_u		
5.7	5.5	$5e_g \rightarrow 8a_{2u}(^1E_u)$	$^1A_{2u}$	$^1A_{2u}$	$^1A_{2u}$

[a] Reference 16. [b] P. Day, M. J. Smith, and R. J. P. Williams, *J. Chem. Soc. A*, 668 (1968). [c] D. S. Martin, Jr., *Inorg. Chim. Acta Rev.*, **5**, 107 (1971). [d] Forbidden L → M ($2a_{2g} \rightarrow 8b_{1g}$) transitions also anticipated in this region. [e] Onset of absorption to shoulder of the 5.7-eV peak. [f] $^3E_g' + {}^3A_{1g}' + {}^3A_{2g}' + {}^3B_{1g}' + {}^3B_{2g}'$; see text.

pared to the experimental results of spectral studies of this complex ion in solution and in the K_2PtCl_4 salt. In this table only the calculations of the d → d and allowed charge transfer transitions are compared to experiment. As noted before, regarding Figure 1, there are ligand levels, namely the $2a_{2g}$ and $13e_u$ levels, which are energetically in the same region as the d orbitals. Electrons in the $2a_{2g}$ level could be involved in "forbidden transitions" to the $8b_{1g}$ level which would be close in energy to the d → d transitions, which are also "forbidden." This forbidden charge transfer transition would obtain its intensity from a vibronic mechanism, coupling in fact to an e_u vibrational mode which is responsible for the intensity of the d → d transition, $5b_{2g} \rightarrow 8b_{1g}$. Thus the present calculation, unlike previous theoretical work, suggests that there may be additional complications in the interpretation of the optical spectra of complexes such as $PtCl_4{}^{2-}$ due to forbidden charge transfer transitions arising in the vicinity of traditionally assigned d → d transitions.

In Table II, the symmetry of the excited state involved in a transition from the ground state ($^1A_{1g}$) is given in parentheses after the specification of the one-electron orbitals in the third column. The primes on certain of these symmetry assignments denote that account has been taken of spin–orbit coupling in determining the assignment. In the approximation that the overall wave function of a state is given by the product of orbital functions and spin functions, the symmetry of the total state is given by the product of the irreducible representations of the components. In D_{4h} symmetry the singlet spin function transforms as a_{1g}; hence for singlet states the symmetry designation given is identical with the orbital part. However, the triplet functions transform as a_{2g} and e_g; thus, as indicated in Table II, there are a number of components generated by the product of the orbital and spin parts of the wave function.

It should be emphasized that no explicit calculations of the spin–orbit interaction have been performed; such calculations would yield separate energies for each component but are beyond the scope of the present work. However, it is noteworthy that even without considering spin–orbit coupling, the agreement between theory and experiment is quite reasonable. This is especially the case for the singlet → singlet transitions of the d → d type, where the experimental evidence for the assignments given in Table II is particularly strong. Thus,

work on single crystals of K_2PtCl_4 using polarized light has established that the band at $\sim$3.3 eV appears only in xy polarization. Assuming the vibronic intensity mechanism, in D_{4h} symmetry there is only one transition which can be exclusively xy polarized, the $^1A_{1g} \rightarrow {}^1A_{2g}$ ($d_{xy} \rightarrow d_{x^2-y^2}$). Also recent magnetic circular dichroism (MCD) experiments on $PtCl_4{}^{2-}$ have indicated a distinct "A term" for the band at $\sim$3.7 eV, consistent with a degenerate excited state for at least one of the transitions in the vicinity of the shoulder at $\sim$5.4 eV, consistent with our assignment, $^1A_{1g} \rightarrow {}^1E_u(13e_u \rightarrow 8b_{1g})$. No A term was observed for the band at 5.7 eV; however, a later study of the MCD line shapes in this region suggests that transitions to a degenerate excited state are involved here as well,[35] thus supporting our $^1A_{1g} \rightarrow {}^1E_u$ assignment.

The experimental situation with regard to the very weak bands near 3.0 eV in the $PtCl_4{}^{2-}$ absorption spectrum is much less clear. Indeed, except for the observation of Day, *et al.*,[3] and Interrante and Bundy[36] that the position of the first band (at $\sim$2.6 eV) in K_2PtCl_4 and various PtA_4PtCl_4 salts apparently depends on the metal–metal separation in the solid (suggesting that the transition involved here arises from an out-of-plane d orbital), there is no compelling experimental evidence for any of these assignments. Our identification of the $5e_g \rightarrow 8b_{1g}$ singlet–triplet transition with the 2.6-eV band reflects the above considerations. No transitions were found in the vicinity of the 2.2 eV experimental absorption band, which is extremely weak but has been observed both in solution and solid-state spectra. This band may arise from spin–orbit effects, which have not been explicitly considered in this calculation or may be even spurious. In total, the agreement with experiment must be considered remarkable especially in view of the neglect of spin–orbit effects, the approximate nature of the calculations, and the fact that relativistic corrections, which one would expect to be quite important for a heavy atom such as Pt, have been ignored. With regard to this latter point it is interesting to note that if it is assumed that the transitions which would show the maximum effect are those which are localized on the Pt atom, then the d → d transitions would be expected to be affected significantly. In particular the $13a_{1g} \rightarrow 8b_{1g}$ transitions should be affected, as the $13a_{1g}$ level contains both Pt 5d and 6s character and the $8b_{1g}$

(35) H. Katô, *Bull. Chem. Soc. Jap.*, **45**, 1281 (1972).
(36) L. V. Interrante and F. P. Bundy, *Inorg. Chem.*, **10**, 1169 (1971).

Table III. Theoretical and Experimental Transition Energies (in eV) for PdCl₄²⁻

Experiment[a]	Transition-state calculation	Transition	BG[a]	DSW[b]	FM[c]
2.2			³B₁g	³Eg	³A₂g; ³Eg
2.5[d,e]	2.6	$4e_g \rightarrow 7b_{1g}$[f]	¹A₂g	¹A₂g	¹A₂g
2.8[e]	2.5	$4b_{2g} \rightarrow 7b_{1g}(^3A_{1g}' + {}^3E_g')$	¹Eg	¹Eg	¹Eg
	3.2	$11a_{1g} \rightarrow 7b_{1g}(^3B_{2g}' + {}^3E_g')$			³B₁g
3.7	3.5	$4b_{2g} \rightarrow 7b_{1g}(^1A_{2g})$	¹B₁g	¹B₁g	¹B₁g
	3.5	$4e_g \rightarrow 7b_{1g}(^1E_g)$			
	4.3	$11a_{1g} \rightarrow 7b_{1g}(^1B_{1g})$			
4.5	4.3	$10e_u \rightarrow 7b_{1g}(^1E_u)$	¹Eu		¹A₂u
	4.6	$2b_{2u} \rightarrow 7b_{1g}(^1A_{2u})$	¹A₂u	¹A₂u	
	5.4	$10e_u \rightarrow 12a_{1g}(^1E_u)$			
5.6	5.5	$9e_u \rightarrow 7b_{1g}(^1E_u)$	¹Eu		
	5.7	$4e_g \rightarrow 6a_{2u}(^1E_u)$			

[a] Reference 16. [b] Reference 39a. [c] Reference 39b. [d] Weak shoulder observed only in xy polarization. [e] Forbidden L → M ($2a_{2g} \rightarrow 7b_{1g}$) transitions also anticipated in this region. [f] $^3A_{2g}' + {}^3E_g' + {}^3A_{1g}' + {}^3B_{1g}' + {}^3B_{2g}'$; see text.

level contains only Pt 5d character. However, on consulting the tables of Herman and Skillman[37] for relativistic corrections to atomic levels, one finds that the sums of the mass–velocity and Darwin corrections for the Pt 5d and Pt 6s levels are identical with within 0.07 eV, suggesting that such fortuitous cancellations may be also taking place in the molecule and are responsible for the good agreement between theory and experiment.

PdCl₄²⁻. The calculational procedure for PdCl₄²⁻ was exactly analogous to that for PtCl₄²⁻. The Pd–Cl bond length was taken as 4.347 bohr; the atomic sphere radii of Pd and Cl and the outer sphere radius were taken as 2.535, 1.811, and 6.160 bohr, respectively. The Watson sphere radius was 6.670 bohr. The value of α for the Pd sphere was 0.70220 and for Cl, 0.72325; the value of α in the inter and outer sphere regions was 0.72020.

The orbital energy level diagram, which results from a spin-restricted solution for PdCl₄²⁻, is shown in Figure 4. The similarity to the PtCl₄²⁻ case is considerable. As for PtCl₄²⁻, there is appreciable covalent interaction between d orbitals and the ligand orbitals. Also the d-orbital ordering is the same: $7b_{1g}(d_{x^2-y^2}) > 4b_{2g}(d_{xy}) > 4e_g(d_{xz},d_{yz}) > 11a_{1g}(d_{z^2})$. Even the wave functions of the valence orbitals are qualitatively very similar. This is consistent with the conclusion, reached earlier on the basis of nuclear quadrupole resonance data,[38] that the charge distributions in these two ions are closely similar. Here, however, the intermixing of d-like and ligand-like orbital energy levels is even more pronounced than in the PtCl₄²⁻ case. In particular, three ligand levels fall within the energy range of the three occupied d levels, and the $2a_{2g}$ is within 0.17 eV of the highest occupied MO.

In Table III, the calculated transition-state energies for d → d transitions and allowed charge transfer transitions are listed and compared to the experimental values. In this table as in Table II, the primes on the symmetry assignments of various excited states involved in transitions are used to denote the fact that spin–orbit coupling has been considered in making the assignments.

The numerical agreement between the energies of the experimental absorption peaks and the calculated transition-state energies as shown in Table III is quite

(37) F. Herman and S. Skillman, "Atomic Structure Calculations," Prentice-Hall, Englewood Cliffs, N. J., 1963.
(38) K. Ito, D. Nakamura, Y. Kurita, K. Ito, and M. Kubo, J. Amer. Chem. Soc., 83, 4526 (1961); E. P. Marram, E. J. McNiff, and J. L. Ragle, J. Phys. Chem., 67, 1719 (1963).
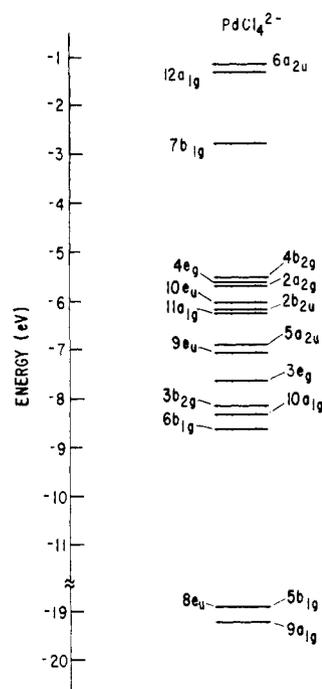
Figure 4. Ground-state SCF-Xα electronic energy levels of PdCl₄²⁻ in the approximate stabilizing electrostatic field of the K₂PdCl₄ crystalline environment. The highest occupied orbital is $4b_{2g}$.

good. However, the assignments differ in several respects from those given previously (compare column 3 with columns 4 and 5).

The main area of disagreement is with regard to the origin of the bands near 2.8 and 3.7 eV. The previous treatments have assigned these bands to spin-allowed d → d type transitions, mainly on the basis of comparisons with the spectra of the PtCl₄²⁻ complex as well as limited information obtained from polarized absorption spectra[39] and magnetic circular dichroism data.[10]

It has generally been assumed, in this earlier work, that the "d" orbitals are sufficiently well separated in energy from the "ligand" orbitals, so that the ligand → metal (L → M) transitions occur at substantially higher energy; however, the results of Figure 4 suggest that this may not be the case for the PdCl₄²⁻ ion. There-

(39) (a) P. Day, M. J. Smith, and R. J. P. Williams, J. Chem. Soc. A, 668 (1968); (b) E. Francke and C. Moncuit, C. R. Acad. Sci., Ser. B, 271, 741 (1970).

fore, the possibility of the bands in this region arising from both d → d and forbidden L → M charge transfer transitions such as $2a_{2g} \rightarrow 7b_{1g}$ must be considered. This could account for the moderate intensity of the "bands" near 2.8 eV[39] for which our calculations suggest singlet → triplet transition assignments.

Indeed, the experimental evidence regarding the transitions in this region is by no means unambiguous. Comparison with the spectra of the $PtCl_4^{2-}$ complex suggests a similar sequence of transitions shifted to lower energy in the case of $PdCl_4^{2-}$. Such a shift is consistent with the anticipated smaller "ligand field splitting" for palladium as compared to platinum. This is qualitatively what our transition-state calculations on these ions show (compare Tables II and III); however, for most of the d → d type transitions, the amount of this shift is appreciably less than has been suggested previously.

In the particular case of the $^1A_{1g} \rightarrow {}^1A_{2g}$ transition, the previous assignments place this at 2.5 eV in $PdCl_4^{2-}$ where a weak shoulder has been observed in the xy polarized spectrum.[39] This is ~0.8 eV below the corresponding assignment for $PtCl_4^{2-}$. Our calculations instead identify the shoulder at 2.5 eV with a $^3A_{2g}{}'$ component of the "^3E_g" state split by spin–orbit coupling and indicate little or no shift in the position of the $^1A_{1g} \rightarrow {}^1A_{2g}$ transition from Pt to Pd.

Similarly, the observation of an MCD A-term in the vicinity of the 2.8-eV band[10a] could be accounted for by means of a degenerate $^3E_{1g}{}'$ state also produced by spin–orbit coupling. Such spin–orbit splitting of triplet excited states, along with the possibility of symmetry forbidden L → M transitions, considerably complicates the interpretation of the optical spectrum in this region.

The situation with regard to the more intense charge transfer type bands above 4 eV is fortunately somewhat more straightforward. In the case of the 5.6-eV band, MCD results strongly suggest a $^1A_{1g} \rightarrow {}^1E_u$ assignment and both MCD and spectral reflectance data indicate

probable $^1A_{1g} \rightarrow {}^1A_{2u}$ and $^1A_{1g} \rightarrow {}^1E_u$ transitions in the vicinity of the 4.5-eV band.[10a]

Summary

A good description of both the optical and X-ray photoemission spectra of $PtCl_4^{2-}$ and $PdCl_4^{2-}$ has been obtained on the basis of the molecular orbital energy level diagrams of Figures 1 and 4 and the transition state concept. This is in distinct contrast to recent *ab initio* LCAO approximate Hartree–Fock calculations on $CuCl_4^{2-}$[18] and $Ni(CN)_4^{2-}$[23,24] which maintain that Koopmans' theorem is not valid for such systems and that one can no longer discuss complexes of this type on the basis of a molecular orbital scheme.

It is important to appreciate the fact that the present SCF-Xα-SW method, although clearly capable of yielding results which are in substantial quantitative agreement with experiment in its present form, is still susceptible to improvements and modifications, within its basic structure. It is possible that a different set of atomic α's may prove to be better practically and theoretically more justified.[40] Overlapping atomic spheres which provide a simple means of incorporating non-muffin-tin corrections to the potential may also prove useful for systems such as those treated here (see following paper). Explicit spin–orbit coupling calculations using the wave functions generated from an Xα-SW calculation would also be very desirable for systems containing heavy metal atoms.

Thus, in spite of the fact that this present work represents the most accurate MO calculations to date on such heavy metal systems, there is certainly room for future improvements.

(40) J. C. Slater, *Int. J. Quantum Chem.*, 7S, 533 (1973).